ELECTROMAGNETIC RESPONSE OF HUMAN BEING BEHIND A WALL BARRIER

Kedar Nath Sahu
Department of Electronics and Communication Engineering
Stanley College of Engineering and Technology for Women, Hyderabad, India

Abstract*—Detection of the respiration rate and/or heartbeat rate are very important for both radar based lie-detection and life-detection. In the existing literature, it is observed that detection of heartbeat signals is done by using some microwave setup and experimental results about respiration and heartbeat rate have been obtained. Also the microwave heart signal has been mathematically modeled from a signal processing point of view or simulated in a general sense without considering electromagnetic properties of body tissues like bone, flesh, skeleton etc. surrounding the heart. In this paper, electromagnetic modeling of human body is presented and some theoretically estimated results for heart reflection coefficient, sensitivity and dynamic range of radar system using the microwave radiation from an ultra-wideband frequency-modulated continuous-wave (UWB FMCW) radar with frequency sweep from 1-11 GHz located at a distance of one meter away from the subject are presented. This estimation shall be useful in the design of a radar system for heartbeat detection related applications like lie detection, life detection of human being buried under the debris of earthquake rubble and see-through-the-wall (STTW) search operations.

Index Terms—**Lie-detection, Life-detection, Polygraph, Reflection coefficient, Radar sensitivity, Power budget, Dynamic range.**

I. INTRODUCTION

Lie-detection and life-detection are the two major concerns that require the remote detection and/or monitoring of cardio-pulmonary features of a human being.

1.1. Lie-detection

The need for lie-detection is to resolve disputes that spring up over inheritance, forgery, impersonation as well as for forensic applications. Of all the existing methods for lie-detection, polygraph testing has been used very popularly. The underlying theory of the polygraph is that when people lie they also get measurably nervous. The heartbeat increases, blood pressure goes up, breathing rhythms change, perspiration increases, etc. A baseline for these physiological characteristics is established by asking the subject questions whose answers the investigator knows. Deviation from the baseline for truthfulness is taken as the sign of lying. Thus as deliberate lying produces bodily reactions reflected in blood pressure, breath and heart rates etc., a polygraph ("lie-detector") testing instrument simultaneously measures and records physiological changes caused by the sympathetic nervous system through the couplings to the body of the person while the subject is asked a series of questions for which he has to answer 'yes' or 'no'.But the method suffers from the problems that it does not have scientific validity. The machine measures changes in blood pressure, breathe rate and respiration rate and from these data a trained expert detects whether the person is lying. But these can also be caused by many causal factors like nervousness, anger, sadness, embarrassment, fear and number of medical conditions such as colds, headaches, constipation, or neurological and muscular problems and hence polygraph test may lead to inaccurate lie detection. Also the method suffers from the problem of countermeasures. The effectiveness or better accuracy of polygraph test could be guessed if it would have been stealthiest. Later, a few new techniques such as functional-Magnetic Resonance Imaging (f-MRI), Brain Fingerprinting were emerged. But all of these techniques require the consent of the person to be examined and therefore such techniques whether justifiable or not, invade the privacy of someone's mind and therefore are invasive methods. Recent advances in radar technology promise to bring lie-detection technique far beyond the notoriously unreliable polygraph. An ultra-wideband (UWB) radar based lie-detector was proposed by Enrico M. Staderini in 2002.This was the first radar based lie-detector which could perform remote, unobtrusive, non-invasive and stealthy lie detection. This bears no psychological discomfort and problems of countermeasures could be overcome.

1.2. Life-detection

Life-detection is necessary when human victims are trapped deep under earthquake rubble or collapsed building debris. Many microwave-based life detection systems have been developed to locate the human victims through detection of breathing and heartbeat signals. The conventional methods for life detection viz. utilization of dogs, seismic or optical devices, acoustic devices such as geophones and the rescue robot were not effective due to their own limitations. This gave rise to the need for remotely observing the physiological status of passive victims who are completely trapped or too weak to respond to existing conventional rescue systems.

II. LITERATURE SURVEY

A summary of the existing methods for both lie detection and life detection found in the literature are presented below.In addition to the popular polygraph testing, some new techniques such as functional-MRI (f-MRI) and brain fingerprinting presented by Yogender S. Bansal et al. [1] were used in numerous cases of lie detection.

The first non-invasive lie-detection technique was proposed in 2002 when Enrico M. Staderini presented the concept of the ultra-wideband (UWB) radar based stealthy lie-detector [2] having its experimental setup comprising of an UWB radar and an ECG amplifier. The heartbeat rate of the subject could be detected from a distance of 5cm from the thorax. The mean heart period was yielded to be of 712.9 ms i.e. 1.4Hz.

So far as the microwave life-detection systems are concerned preliminary methods [3-5] used in 1970s for microwave cardiograph, microwave interferometers etc. have limited use for short distances less than 1m only. These conventional short-range, contactless radar techniques used to remotely detect breath and heart rates were limited to children under a few years of age. Microwave life detection system operating at 10 GHz (X-band) [6] was developed in 1986 which didn't penetrate sufficiently deep. An automatic clutter canceler [7] for

microwave life detection system was presented in 1991 byChang et al. Then microwave life-detection systems using L or S-band [8] operating at 1150 MHz or 450 MHz were developed in 2000 which could detect the breathing and heartbeat signal of human subjects through an earthquake rubble or a construction barrier of about 10ft. thickness. Recently, another light-weight rescue radar system was proposed in 2011 by M. Donelli [9] which was based on continuous-wave (CW) X-band radar for extraction of heartbeat fluctuations using independent component analysis (ICA) algorithm to mitigate noise and clutter related issues. A See-Through-The-Wall (STTW) imaging radar using UWB short-pulse radar system was developed in 2005 [10] to operate at 10 GHz. Then in 2007 use of basic compact Doppler and ultra-wide band (UWB) radar were exploited for see-through-the-wall (STTW) life detection and monitoring applications [11] and are seen to penetrate barriers of higher density materials like RCC blocks, sheetrock, brick, wood, plastic, tile, fiberglass etc. One ultra-wideband frequency modulated (UWB FM-CW) radar operating at L- or S- band with an extended sweep from 0.5 to 8 GHz was an innovation in the detection of human beings walking or just moving behind a wall [12] when N. Mareff, P. Millot et.al presented the modeling of wall attenuation incorporating electromagnetic properties of typical building materials. As an extension of this work, they computed the power budget and system dynamic range by evaluating the frequency dependent radar cross section (RCS) of human being [13]. In 2011, a life-detection system operating at L-band and using a microprocessor based automatic clutter cancellation subsystem [14] was proposed by N. Gauri et.al.

Thus in the literature, the potential use of radars ranging from the most basic continuous-wave (CW) Doppler radars to ultra-wideband (UWB) radars for biomedical, clinical, defense, forensic, search and rescue applications have been described. An overview of the chronological developments under various categories has been presented in [15]. The clutter related issues were dealt using the algorithms described in [16, 17].

From the above analysis regarding both forensic and lifesaving applications (i.e. lie detection and life detection respectively), the fundamental objective is to detect the heart and breathing signals that modulate the radar signal. Various experimental setups, operating frequencies, mathematical models, algorithms have been developed to accomplish the ultimatum. Moreover, propagation medium loss, hardware regulations and probability of detection also affect transmit power levels, frequencies, and modulation choices, ultimately limiting the effectiveness of any radar. Therefore care must be taken in the design of a suitable radar transceiver such that the component of transmitter power to be incident on the sensitive heart element is well within a safe limit, without causing any danger to the functioning of heart. As heart is surrounded by the body parts of different dielectric characteristics and as electromagnetic wave (EMW) propagation is dependent on the medium, focus shifted to the use of the human tissue properties in building different models [18-20]. In this paper, incorporation of the electromagnetic properties of different body parts has been proposed in the design of a radar system that can be effectively used for heartbeat detection.

III. THEORETICAL BACKGROUND

In order to study the behavior of the backscattered field from a human body illuminated by plane electromagnetic waves of a radar transmitter, we simplify the problem by modeling the human body as a series of biological tissue layers of complex permittivity. Knowing the permittivity of the tissue materials, and by utilizing the basic principles of electromagnetic wave propagation in accordance with the physical processes that determine the speed of propagation and the amount of attenuation, the power received by the radar receiver, the electric field (E-field) reflection coefficients at every interface and power reflection coefficient of the heart can be determined.

3.1. Electromagnetic Modeling of Human Body

The radar based methods for both lie-detection and life-detection deals with a person sitting or lying still but has his chest moving due to two main causes: respiration and heartbeat. In order to model the response of human body to radar waves, it is necessary to know with enough precision the electromagnetic characteristics of typical biological tissues used to build the body. For this purpose, the transverse section of human anatomy was referred. Figure 1 depicts the transverse section of human thorax showing the contents of the middle and the posterior mediastinum. The pleural and pericardial cavities are exaggerated since normally there is no space between parietal and visceral pleura and between pericardium and heart. Various tissues like sternum, hard cholesterol, muscle, ribs, costal pleura, pleural cavity, pulmonary pleura, pericardium cavity, heart, pulmonary artery (left and right), aorta, internal mammary vessels, thoracic aorta, esophagus, bronchus, thoracic duct, body of thoracic vertebrae, lungs (left and right) etc. encounter in the path of propagation partly or fully, when the human body is illuminated by the radar wave.

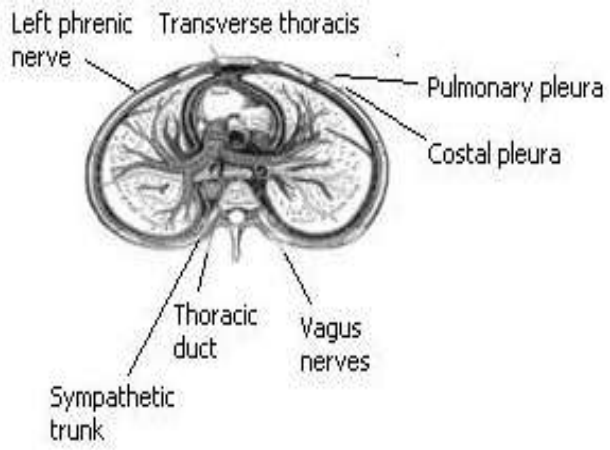

Figure 1. Transverse section of the human thorax.

Let us consider only some of the major biological tissues such as skin, fat, muscle, ribs and heart as the fundamental layers for a simple modeling of human body. As electromagnetic behavior due to heartbeat movements are of interest, assuming the radiation exposure from anterior of the human body to the posterior through heart, the complete tissue structure in view of the electromagnetic modeling of the complete human torso is considered as shown in Figure 2.

Skin	Hard Cholesterol	Muscle	Ribs	Heart	Ribs	Muscle	Hard Cholesterol	Skin

Figure 2. Complete tissue structure for EM modeling of human torso.

The electromagnetic properties of tissues corresponding to the center frequency, 6 GHz of a 1-11 GHz ultra-wideband frequency-modulated continuous-wave (UWB FM-CW) radar modeling as mentioned in [21] have been shown in Table 1. For hard cholesterol and ribs, properties of fat and bone cortical have been considered respectively. For skin, property of skin (dry) and not of skin (wet) is taken into consideration.

As the thicknesses of tissues vary for different persons within a normal range, average thickness for each tissue has been considered in the analysis.

Table 1. Electromagnetic properties and thickness values of human tissues at 6 GHz frequency.

Tissue name	Dielectric constant	Conductivity	Thickness (mm)	Average Thickness (mm)
Skin	34.946	3.8912	1 – 1.5	1.25
Hard Cholesterol (Fat)	4.9367	0.30623	4 - 10	7
Muscle	48.217	5.2019	6 - 14	10
Ribs (Bone Cortical)	9.5869	1.2026	15	15
Heart	48.62	6.1223	12	12

Assuming free space over the distance of one meter between the radar and the human subject, the complete medium of propagation can be realized by considering all the constituent tissues in the same sequence as shown in Figure 2 with free space from the anterior skin surface up to one meter till the position of radar. Of course, free space covered on the posterior side need not be specified.

Using the concept of wave propagation in dielectrics as found in [22], the characteristic impedance of a medium is given by,

$$\eta = \sqrt{\frac{j\omega\mu}{\sigma + j\omega\varepsilon}} \tag{1}$$

As human body tissues are almost non-ferrous, the magnetic response is usually very weak compared to dielectric response for wave propagation and therefore, in order to start with a simple analysis, for such tissue materials we may assume conductivity, $\sigma = 0$ and $\mu_1 = \mu_0 = \mu_2$ considering any two tissues as two mediums and thus characteristic impedance becomes,

$$\eta = \sqrt{\frac{j\omega\mu}{j\omega\varepsilon}} = \sqrt{\frac{\mu}{\varepsilon}} \tag{2}$$

Characteristic impedances of the two mediums can be given as

$$\eta_1 = \sqrt{\frac{\mu_1}{\varepsilon_1}} \tag{3}$$

and $$\eta_2 = \sqrt{\frac{\mu_2}{\varepsilon_2}} \tag{4}$$

Therefore the ratios, $$\frac{\eta_1}{\eta_2} = \frac{\sqrt{\varepsilon_{r_2}}}{\sqrt{\varepsilon_{r_1}}} \tag{5}$$

and $$\frac{\eta_2}{\eta_1} = \frac{\sqrt{\varepsilon_{r_1}}}{\sqrt{\varepsilon_{r_2}}} \tag{6}$$

In general, considering a multi-layer system and assuming normal incidence [23], the E-field reflection coefficient of n-th layer can be given by

$$\Gamma_n = \frac{E_{n_r}}{E_{n_i}} = \frac{\sqrt{\varepsilon_r^n} - \sqrt{\varepsilon_r^{n+1}}}{\sqrt{\varepsilon_r^n} + \sqrt{\varepsilon_r^{n+1}}}, \tag{7}$$

where Γ_n is the reflection coefficient of the interface n between the layers n and $n + 1$; ε_r^n and ε_r^{n+1} are the relative permittivity of layers, n and n+1 respectively according to the concept of reflection of uniform plane waves at normal incidence [22]. The electric field (E-field) reflection coefficients during forward propagation for every interface between consecutive layers are obtained and shown in Table 2.

Table 2. E-field reflection coefficients for forward propagation.

Interface Number, n	Interface between layers n and n+1	Reflection Coefficient, Γ_n
1	Free space and Skin	-0.7106
2	Skin and Hard Cholesterol (Fat)	-0.4536
3	Hard Cholesterol(Fat) and Muscle	-0.5152
4	Muscle and Ribs	-0.3832
5	Ribs and Heart	-0.3850
6	Heart and Ribs	-0.3850
7	Ribs and Muscle	-0.3832
8	Muscle and Hard Cholesterol(Fat)	-0.5152
9	Hard Cholesterol(Fat) and Skin	-0.4536
10	Skin and Free space	-0.7106

As expected, it is observed from Table 2 that of any two consecutive tissue mediums where $\varepsilon_r^1 < \varepsilon_r^2$, the electric field is reflected with change of sign, and reverse is the case if $\varepsilon_r^2 < \varepsilon_r^1$. Signs of transmitted electric fields are the same as those of the incident wave irrespective of whether ε_r^1 is greater or less than ε_r^2.

IV. Power Relations

Using the following power relations obtained in [22] as a general rule for average power transfer per unit area through reflection and transmission about an interface separating two lossless dielectric regions 1 and 2, incident, reflected and transmitted power for every interface can be determined.

$$\text{Net incident power, } P_i^+ = \frac{(E_1^+)^2}{2\eta_1} \tag{8}$$

$$\text{Net reflected power, } P_r^- = |\Gamma|^2 P_i^+ \tag{9}$$

$$\text{Net transmitted power, } P_t^+ = \left(1 - |\Gamma|^2\right) P_i^+ \tag{10}$$

V. Power Calculations

When the power carried by the radar wave is incident on any interface, n separating the two tissue mediums n and n+1, known as incident power during forward propagation, P_{ni}^+, part of it is transmitted in the same forward direction, known as transmitted power, P_{nt}^+ and the remaining power is reflected in the backward direction known as reflected power component during forward propagation, P_{nr}^-. Amount of power reflected from every interface keeps getting retransmitted again in a backward propagation mode and is finally received at the receiver. Such retransmitted power components from each of the interfaces received by the radar receiver in a backward propagation mode will be known as reflected power component during backward propagation, $(P_{nr}^-)'$. In this work, the above power components are first obtained by assuming a lossless propagation to observe the basic propagation characteristics and then they are recalculated separately for a lossy propagation but this time represented as LP_{ni}^+, LP_{nt}^+ and LP_{nr}^- respectively.

5.1. Lossless Propagation

In the beginning, let us consider tissue mediums as lossless or perfect dielectric, $\varepsilon = \varepsilon'$ (since $\varepsilon'' = 0$ in the equation for complex permittivity, $\varepsilon = \varepsilon' - j\varepsilon''$.

5.1.1. Power calculation for lossless forward propagation

Let the incident power at interface, $n = 1$ is $P_{1i}^+ = P_i$ watts. The incident, reflected and transmitted power at all interfaces in terms P_i watts are listed below in Table 3. The power coefficients are generated by using MATLAB.

Table 3. Incident, reflected and transmitted power for lossless forward propagation in watts.

Interface Number, n	Incident power, P_{ni}^+	Reflected power, P_{nr}^-	Transmitted power, P_{nt}^+
1	P_i	0.5050 P_i	0.4950 P_i
2	0.4950 P_i	0.1019 P_i	0.3931 P_i
3	0.3931 P_i	0.1043 P_i	0.2888 P_i
4	0.2828 P_i	0.0424 P_i	0.2464 P_i
5	0.2464 P_i	0.0365 P_i	0.2099 P_i
6	0.2099 P_i	0.0311 P_i	0.1788 P_i
7	0.1788 P_i	0.0263 P_i	0.1525 P_i
8	0.1525 P_i	0.0405 P_i	0.1120 P_i
9	0.1120 P_i	0.0231 P_i	0.0890 P_i
10	0.0890 P_i	0.0449 P_i	0.0440 P_i

The coefficients of the above power values are again obtained in terms of decibels as shown in Table 4 by using MATLAB for easy graphical representation.

Table 4. Incident, reflected and transmitted power coefficients in decibels for lossless forward propagation.

Interface Number, n	Incident power, P_{ni}^{+} (dB)	Reflected power, P_{nr}^{-} (dB)	Transmitted power, P_{nt}^{+} (dB)
1	0	-2.9672	-3.0539
2	-3.0539	-9.9196	-4.0545
3	-4.0545	-9.8154	*-5.3941*
4	-5.3941	-13.7251	-6.0839
5	-6.0839	-14.3748	-6.7806
6	-6.7806	-15.0715	-7.4773
7	-7.4773	-15.8083	-8.1671
8	-8.1671	-13.9279	-9.5066
9	-9.5066	-16.3724	-10.5073
10	-10.5073	-13.4744	-13.5612

The graphical representations of these incident, reflected and transmitted power coefficients in decibels for lossless forward propagation are shown in Figure 3 (a), (b) and (c) respectively.

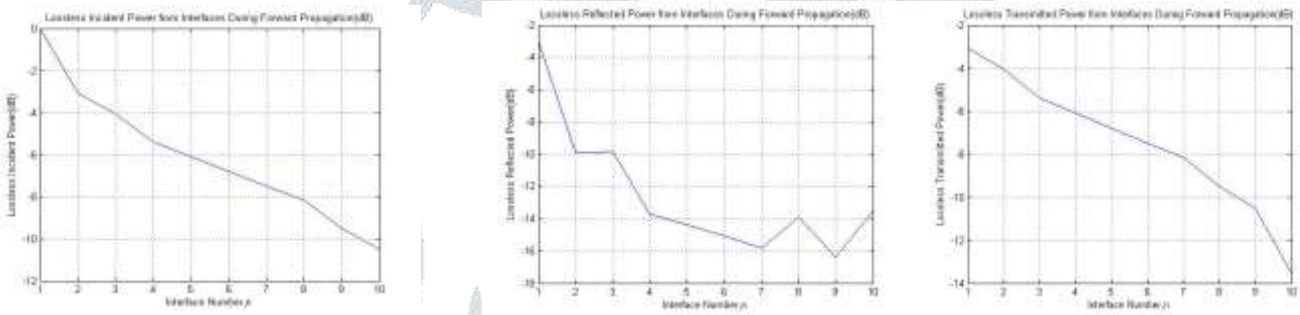

3(a) 3(b) 3(c)

Figure 3. (a) Incident (b) reflected and (c) transmitted lossless power for forward propagation in decibels

From Figure 3, it is observed that the amplitudes of powers decrease with the progress of the wave.

5.1.2. Power calculation for lossless backward propagation

The reflected power components during backward propagation $(P_{nr}^{-})'$ are obtained in terms P_i watts and the coefficients are expressed also in terms of decibels as shown in Table 5.

Table 5. Reflected power from various interfaces during backward propagation.

Interface Number, n	1	2	3	4	5	6	7	8	9	10
$(P_{nr}^{-})'$in watts	0.5050	0.0504	0.0410	0.0122	0.0090	0.0065	0.0047	0.0062	0.0026	0.0040
$(P_{nr}^{-})'$in dB	9672	2.9735	3.8699	9.1192	0.4586	1.8521	3.2857	2.0950	5.8790	3.9817

The plot of the reflected power coefficients during backward propagation $(P_{nr}^{-})'$expressed in dB as above is shown in Figure 4.

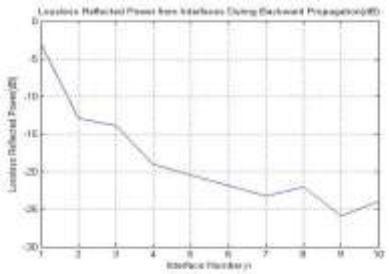

Figure 4. Lossless reflected power during backward propagation in dB.

5.2. Lossy Propagation

In reality, body tissues are lossy dielectric and the amount of loss depends on the magnitude of loss tangent, $\varepsilon''/\varepsilon'$ where $\varepsilon'' = \frac{\sigma}{\omega}$. Therefore the loss tangent is equal to $\sigma/\omega\varepsilon'$ and has a direct influence on the attenuation coefficient, α. The attenuation coefficient, α expressed in Neper/m and power attenuation factor, $e^{-2\alpha x}$; x being the average tissue thickness for all body tissues are calculated using MATLAB and listed in Table 6.

Table 6. Attenuation coefficients and attenuation factors for body tissues.

Interface Number, n	1	2	3	4	5	6	7	8	9	10
Interface between layers n and n+1	Free Space	Skin (Dry)	Hard Cholesterol (Fat)	Muscle	Ribs	Heart	Ribs	Muscle	Hard Cholesterol (Fat)	Skin (Dry)
Attenuation coefficient (Np/m)	0	122.8538	25.8990	9.9025	.3021	53.4312	2.3021	39.9025	25.8990	122.8538
Power attenuation factor	1	0.7356	0.6959	0609	1143	0.0198	.1143	.0609	0.6959	0.7356

5.2.1. Lossy power calculation during forward propagation

By multiplying the corresponding attenuation factor with the transmitted power through every interface and then using the general rule for reflection and transmission, the lossy incident, reflected and transmitted power values were first obtained at all interfaces in terms of P_i watts as shown in Table 7 and then, because all of these lossy powers were too small values for graphical representation they were represented in decibels as shown in Table 8.

Table 7. Incident, reflected and transmitted lossy power at all interfaces in watts.

Interface Number, n	Lossy Incident power, LP_{ni}^{+}	Lossy Reflected power, LP_{nr}^{-}	Lossy Transmitted power, LP_{nt}^{+}
1	P_i	0.5050 P_i	0.4950 P_i
2	0.3641 P_i	0.0749 P_i	0.2892 P_i
3	0.2012 P_i	0.0534 P_i	0.1478 P_i
4	0.009 P_i	0.0013 P_i	0.0077 P_i
5	8.7815e-04 P_i	1.3016e-04 P_i	7.4799e-04 P_i
6	1.4806e-05 P_i	2.1946 e-06 P_i	1.2612e-05 P_i
7	1.4413e-06 P_i	2.1167e-07 P_i	1.2296e-06 P_i
8	7.4921e-08 P_i	1.9885e-08 P_i	5.5036e-08 P_i
9	3.8298e-08 P_i	7.8815e-09 P_i	3.0417e-08 P_i
10	2.2373e-08 P_i	1.1298e-08 P_i	1.1075e-08 P_i

Table 8. Incident, reflected and transmitted lossy power at all interfaces in decibels.

Interface Number, n	Lossy Incident power, LP_{ni}^{+} (dB)	Lossy Reflected power, LP_{nr}^{-} (dB)	Lossy Transmitted power, LP_{nt}^{+} (dB)
1	0	-2.9672	-3.0539
2	-4.3877	-11.2535	-5.3884
3	-6.9631	-12.7239	-8.3026
4	-20.4544	-28.7854	-21.1442
5	-30.5643	-38.8552	-31.2610
6	-48.2956	-56.5865	-48.9923
7	-58.4124	-66.7435	-59.1022
8	-71.2540	-77.0148	-72.5935
9	-74.1682	-81.0339	-75.1689
10	-76.5027	-79.4699	-79.5566

The above lossy incident, reflected and transmitted power coefficients in decibels are generated by using MATLAB and plotted as shown in Figure 5.

(a) (b) (c)

Figure 5. (a) Incident (b) reflected and (c) transmitted lossy power for forward propagation in decibels.

5.2.2. Lossy power calculation during backward propagation

The reflected lossy power components during backward propagation $(LP_{nr}^{-})'$ are obtained in terms P_i watts and the coefficients are expressed in terms of decibels as shown in Table 9.

Table 9. Reflected lossy power from all interfaces during backward propagation.

Interface Number, n	1	2	3	4	5	6	7	8	9	10
$\left(LP_{nr}^{-}\right)'$ in dB	9672	5.6412	9.6870	9.2398	9.4195	)4.8821	25.1559	48.2688	55.2021	55.9726

The plot of the reflected lossy power coefficients during backward propagation $(LP_{nr}^{-})'$expressed in dB as above is shown in Figure 6.

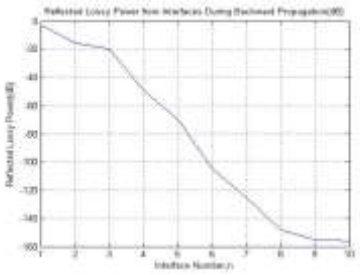

Figure 6. Lossy reflected power during backward propagation in dB.

VI. HEART REFLECTION COEFFICIENT, MINIMUM DETECTABLE SIGNAL AND DYNAMIC RANGE

Power reflection coefficient, Minimum Detectable Signal (or radar sensitivity) and Dynamic Range are some of the vital parameters in the design of any radar system. These terms are first defined and then evaluated for both cases of lossless and lossy propagation in our work. Heart reflection coefficient is the ratio of power incident on heart wall (n=5) to the total power incident on heart wall during forward propagation. Minimum Detectable Signal (MDS) refers to the radar sensitivity and is equal to the lowest of all the reflected power values from various interfaces received at the radar receiver. Dynamic range of radar system i.e. System Dynamic Range (SDR) is the ratio of the power of radar transmitter to the minimum detectable signal. Similarly, the required dynamic range for the radar receiver can be fixed by the ratio between the strongest received signal and the smallest target response [13]. Thus the receiver dynamic range for the UWB FM-CW radar, in this work, is determined by the ratio of the power received from the chest wall of the subject and the power received from the heart wall. The above radar design parameters are evaluated as below for both lossless and lossy mediums.

6.1. Results

The above design parameters such as heart reflection coefficient, minimum detectable signal and system dynamic range are obtained as below for lossless and lossy propagation.

6.1.1. Lossless propagation

We have already obtained the power reflected from heart wall (n=5) during forward propagation as P_{5r}^{-}=0.0365P_i and total power incident on heart wall as P_{5i}^{+}=0.2464P_i.Thus power reflection coefficient of heart can be obtained as

$$RC_{heart} = \frac{P_{5r}^{-}}{P_{5i}^{+}} = \frac{0.0365P_i}{0.2464P_i} = 0.1482 \text{ or } -8.291 \text{ dB}$$

Minimum detectable signal = minimum of all values of $(P_{nr}^{-})'$ (from n=1 to 10) =$(P_{9r}^{-})'$= 0.0026P_i i.e. 4.121dBm when P_i=1Watt.
System dynamic range (SDR) for lossless propagation can be obtained as

$$\text{SDR} = \frac{P_i}{0.0026P_i} = 387.1691 \text{ i.e. } 25.88 \text{ dB}$$

Now, receiver dynamic range (RDR) for lossless propagation can be obtained by the ratio of the power received from the chest wall i.e. skin surface (n=1) and the power received from the heart wall (n=5) as below.

$$\text{RDR} = \frac{\left(P_{1r}^{-}\right)'}{\left(P_{5r}^{-}\right)'} = \frac{0.505P_i}{0.009P_i} = 56.12 \text{ i.e. } 17.49 \text{ dB}$$

6.1.2. Lossy propagation

Similarly, lossy power reflected from heart surface (n=5) during forward propagation is obtained as $LP_{5r}^{-} = 1.3016e-04P_i$ and total power incident on heart surface $LP_{5i}^{+} = 8.7815e-04P_i$.Thus lossy power reflection coefficient of heart can be obtained as
Minimum detectable signal = minimum of all values of $(LP_{nr}^{-})'$ (from n=1 to 10)

$=(LP_{10r}^{-})'$= 2.5278 e $-$ 016P_i i.e.-125.97 dBm when P_i=1Watt.

System dynamic range for lossy propagation can be obtained as

$$RC_{heart} = \frac{LP_{5r}^{-}}{LP_{5i}^{+}} = \frac{1.3016e-04P_i}{8.7815e-04P_i} = 0.1482 \text{ i.e. } -8.291 \text{ dB}$$

Minimum detectable signal = minimum of all values of $(LP_{nr}^{-})'$ (from n=1 to 10)
$=(LP_{10r}^{-})'= 2.5278\ \mathrm{e}-016P_i$ i.e.-125.97 dBm when P_i=1Watt.

System dynamic range for lossy propagation can be obtained as

$$\mathrm{SDR}=\frac{P_i}{2.5278e-16P_i}=3.956\mathrm{e}{+15}\ \text{i.e. } 155.97\ \mathrm{dB}$$

Similarly, receiver dynamic range for lossy propagation can be given as,

$$\mathrm{RDR}=\frac{\left(LP_{1r}^{-}\right)'}{\left(LP_{5r}^{-}\right)'}=\frac{0.505P_i}{1.143e-07P_i}=4.418\mathrm{e}{+006}\ \text{i.e. } 66.45\ \mathrm{dB}$$

The radar design parameters such as heart reflection coefficient, minimum detectable signal, system dynamic range and receiver dynamic range obtained separately for both lossless and lossy propagation as above are compared in Table 10.

Table 10. Comparison of design parameters for both lossless and lossy propagation.

Design parameters	Lossless propagation	Lossy propagation
Heart reflection coefficient	-8.291dB	-8.291 dB
Minimum detectable signal (MDS)	4.121 dBm	-125.97 dBm
System dynamic range (SDR)	25.88 dB	155.97 dB
Receiver dynamic range (SDR)	17.49 dB	66.45 dB

Thus from Table 10 it is observed that reflection coefficient of heart is the same in both lossless as well as lossy propagation and is equal to 0.1482 i.e. -8.291 dB.

VII. CONCLUSIONS

Concept of lie-detection and life-detection from the detection of heart and breath rates are effective because heartbeat and respiration related motion cannot be suppressed fully. Also, the propagation of waves through the subject's body is mainly governed by the electromagnetic characteristics of body tissues.

In this paper, a simple one-dimensional electromagnetic model of human body has been presented by incorporating the electromagnetic properties of body tissues corresponding to the midband frequency 6 GHz of a UWB FM-CW radar of frequency bandwidth from 1-11 GHz. The lossless and lossy power coefficients are evaluated during both forward and backward propagation and then their graphical representation is obtained by using MATLAB. The radar is assumed to be located at a distance of one meter from the subject directed toward the upper torso of the subject and the reflection from the heart wall has been quantified. The dynamic range obtained can be taken as a feasible value to meet the system requirements as this quantity in excess of 80 dB is difficult to achieve.The heartbeat signal power derived can be processed further to obtain heartbeat information.

REFERENCES

[1] Yogender S. Bansal, Dalbir Singh, Sreenivas M., Avadh Naresh Pandey. Recent advances in lie detection. J Indian Academy of Forensic Medicine 2004; 26(1), pp. 27-29.

[2] Enrico M. Staderini. An UWB radar based stealthy lie detector.In: Ultra-Wideband Short-Pulse Electromagnetics 6, Edited by Mokole et al., Kluwer Academic/Plenum publishers, 2003, pp. 537-551.

[3] Lin JC, Kiernicki J, Kiernichi M, Wollschlaeger PB. Microwave apexcardiography. IEEE T Microw Theory 1979; 27, pp. 618-620.

[4] Griffin DW. MW interferometers for biological studies. Microwave J 1978; 21, pp. 69-72.

[5] Pedersen PC, Johnson CC, Durney CH, Bragg DG. An investigation of the use of microwave radiation for pulmonary diagnostics. IEEE T Bio-med Eng 1976; 23, pp.410-412.

[6] Chen KM, Misra D, Wang H, Chuang HR, Postow E. An X-band microwave life-detection system. IEEE T Bio-med Eng 1986; 33, pp.697–702.

[7] Chang Huey-Ru, Chen YF, Chen Kun-Mu. Automatic clutter canceler for microwave life-detection systems. IEEE T Instrum Meas 1991; 40(4), pp.747-750.

[8] Chen K, Huang Y, Zhang J, Normal A. Microwave life-detection systems for searching human subjects under earthquake rubble or behind barrier. IEEE T Bio-med Eng 2000; 27, pp.105-114.

[9] Donelli M. A rescue radar system for the detection of victims trapped under rubble based on the independent component analysis algorithm. Prog. Electromagnetic Res Mag 2011; 19, pp.173-181.

[10] Yang Y, Fathy AE. See-through-wall imaging using ultra-wideband short-pulse radar system. IEEE Antennas Propag Soc Intl Sym 2005; 3B, pp.334-337.

[11] Lubecke Victor M, Lubecke Olga Boric, Host-Madsen Anders, Fathy Aly E. Through - the - wall radar life detection and monitoring. Elec & Comp Eng Dept, Knoxville, University of Tennessee, 2007, pp.769-772.

[12] Maaref N, Millot P, Pichot Ch, Picon O. A study of UWB FMCW radar for the detection of human beings in motion inside a building. IEEE T. Geosci Remote 2009; 47(5) , pp.1297-1300.

[13] Maaref N, Millot P, Pichot Ch, Picon O. FMCW ultra-wideband radar for through-the-wall detection of human beings. In: Radar Conference- Surveillance for a Safer World, 2009, RADAR International, 12-16 October 2009; Bordeaux, pp.1-5.

[14] Zade Gauri N, Badnerkar SS. A modern microwave life detection system for human being buried under rubble. Int J Adv Eng Res Stud October-December, 2011; 1(1), pp. 69-77.
[15] Øyvind Aardal, Hammerstad Jan. Medical radar literature overview. Norwegian Defence Research Establishment (FFI) 2010, pp. 1-28.
[16] Petrochilos N, Reznik M, Host-Madsen A, Lubecke V, Boric-Lubecke O. Blind separation of human heartbeats and respiration by the use of a Doppler radar remote sensing. In: IEEE Int Conference on Acoustics, Speech and Signal Processing (ICASSP'07);15-20 April 2007; Honolulu, HI, pp. 333-336.
[17] Byrne W, Flynn P, Zapp R, Siegel M. Adaptive filter processing in microwave remote heart monitors. IEEE T Bio-med Eng 1986; 33, pp.717-722.
[18] Gandhi Om P, Gianluca Lazzi, Furse Cynthia M. Electromagnetic absorption in the human head and neck for mobile telephones at 835 and 1900 MHz. IEEE T Microw Theory 1986; 44(10), pp.1884-1897.
[19] Lawrence C. Chirwa, Paul A. Hammond, Scott Roy, Cumming David RS. Electromagnetic radiation from ingested sources in the human intestine between 150 MHz and 1.2 GHz. IEEE T Bio-med Eng 2003; 50(4), pp.483-492.
[20] Iliana Marinova, Valentin Mateev. Electromagnetic field modeling in human tissue. In: World Academy of Science, Engineering and Technology 2010; 40, pp. 297-30.
[21] Calculation of the dielectric Properties of Body Tissues in the frequency range 10 Hz to 100 GHz. In: Italian National Research Council, Institute for Applied Physics, Florence, Italy.
[22] Hayt WH, Buck JA. Engineering Electromagnetics, 7th ed. India: Tata McGraw-Hill, 2006.

Kedar Nath Sahu, Professor, Department of Electronics and Communication Engineering, Stanley College of Engineering and Technology for Women, Hyderabad, India, received the professional engineering degrees in Electrical Engineering (1996) and Electronics and Communication Engineering (2001) from The Institution of Engineers (India) and M.Tech. (2002) from Visvesvaraiah Technological University, Karnataka, India. He received Ph.D. Degree in Electronics and Communication Engineering from Jawaharla Nehru Technological University Hyderabad (JNTUH), Hyderabad in 2017. He has over 16 years of experience in teaching in the faculty of Electronics and Communication Engineering at various engineering colleges. His research interests include Applied Electromagnetics, Biomedical Engineering, Microwave and Radar Engineering. He is Fellow IETE, IE (India) and Life Member of ISTE.